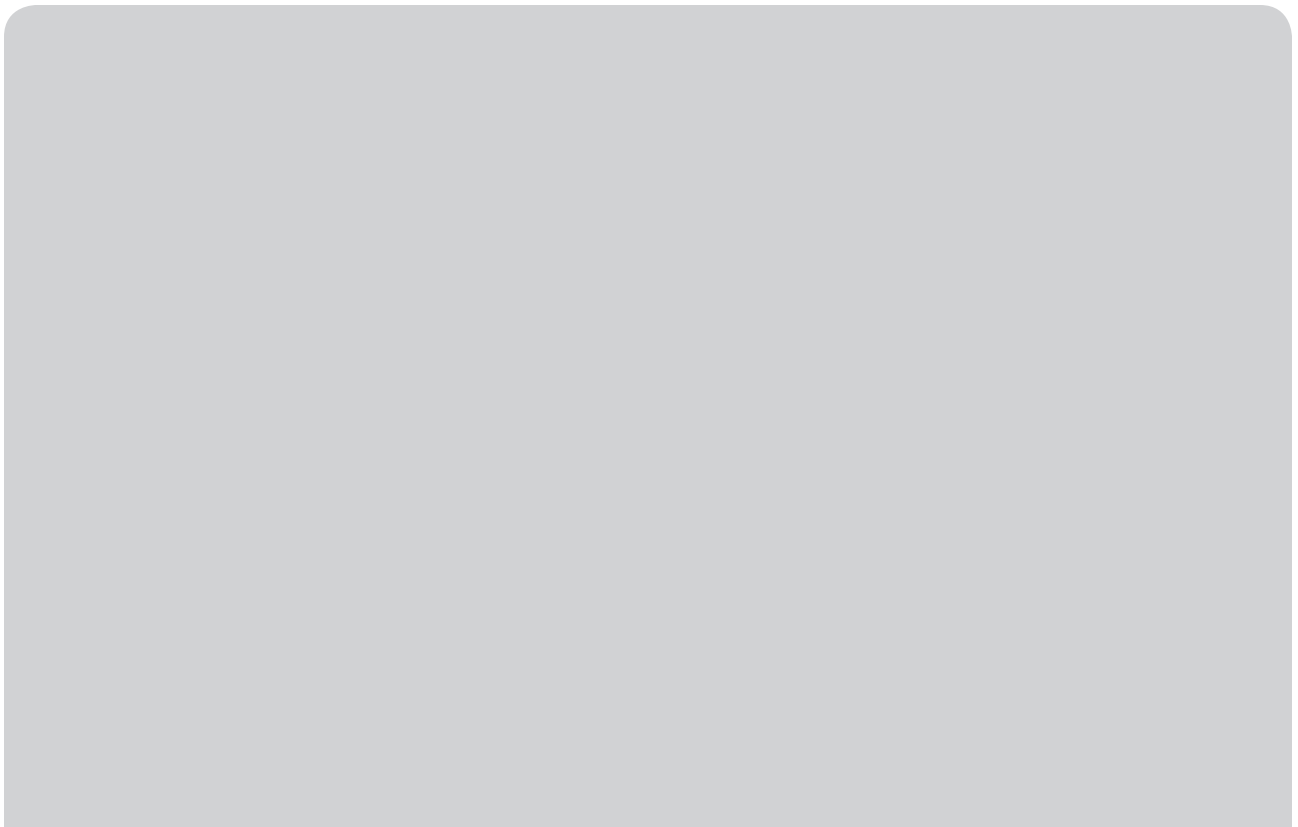


A Case Study of Voltage Transformer Failures

SOLUTION IMPLEMENTATION IN A MODERN DATA CENTER



©PHOTOCREDIT

By Tamer Abdelazim Mellik,
Thomas J. Dionise, and
Robert Yanniello

WHILE PREPARING A MODERN DATA CENTER FOR STARTUP, the commissioning process involved primary circuit switching that resulted in two voltage transformer (VT) failures. As a result, we conducted a comprehensive investigation of the VT failures. As the investigation proceeded, VT ferroresonance on circuit opening and high-frequency switching transients on closing emerged as possible root causes of the failures. After incorporating extensive transient simulations and three rounds of field transient measurements, we designed and implemented a complete solution that included the sizing of

.....
Digital Object Identifier 10.1109/MIAS.2016.2600682
Date of publication: 6 September 2017

snubbers to overcome excessive switching transients and the development of a saturable reactor to protect VTs against the effects of ferroresonance. This article describes the root causes, simulations, field measurements, recommended solutions, and solution implementation for this event. The correlation between field measurements and simulation results shows the effectiveness of modeling the implemented solutions.

Circuit Switching

A commonly performed operation during commissioning or normal facility operation is circuit switching. The switching operation causes transients [1], which can result in equipment damage and danger to personnel who are near the damaged or affected equipment [2], [3]. With the widespread application of vacuum breakers for transformer switching, this phenomenon is receiving renewed attention [4], [5]. The severity of the switching transient voltage (i.e., high magnitude, high frequency, and the damage caused by the transient voltage) are determined by the following circuit characteristics [6], [7]:

- short bus or cable distance between the circuit breaker and transformer
- basic insulation level of the transformer (cast-coil, dry-type, and some oil filled)
- inductance of the load being switched (transformer)
- circuit-breaker switching characteristics: nonsimultaneous operation of poles, current chop (vacuum or SF₆), and restrike (vacuum).

An equally important problem is ferroresonance. ANSI/IEEE Standard 100-1984 [8] defines ferroresonance as “a phenomenon usually characterized by overvoltages and very irregular wave shapes and associated with the excitation of one or more saturable inductors through a capacitance in series with the inductor.” The key elements are saturable inductors in series with capacitance, as shown in Figure 1. In the ferroresonant circuit, the capacitance (XC) can be the capacitance of cable, overhead lines, or stray capacitance of transformer windings or bushings. Under normal operation, XC is smaller than the inductive reactance (XL). However, if some switching event causes the voltage to increase, then the transformer core may be pushed into saturation and the XL lowered. It is possible at some higher voltage that this lower saturated value of XL may equal XC, forming the series resonant circuit called ferroresonance [9]. The ferroresonance phenomenon, as it relates to a VT, is explained in detail in [3].

On 18 November 2013, this data center experienced the failure of two line-end VTs at 24.9 kV in newly installed switchgear. The damage to the line-end VT is shown in Figures 2 and 3. During the investigation, the

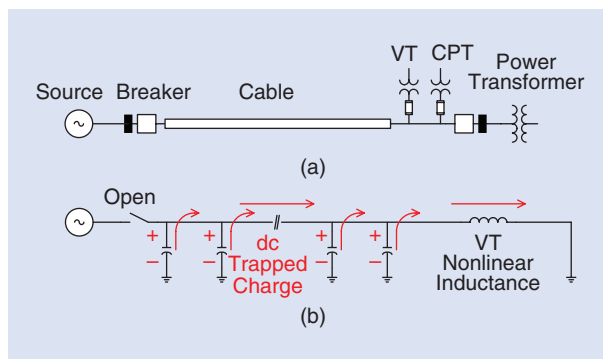


FIGURE 1. A conceptual explanation of VT ferroresonance: (a) a one-line diagram and (b) circuit parameters influencing ferroresonance. VT: voltage transformer; CPT: control power transformer.



FIGURE 2. A line-end VT failure.

bus VTs for the same gear failed on 28 December 2013. The 24.9-kV electrical distribution system for the data center is extensive, with some circuits as long as 800 m, which is partially illustrated in Figure 4. A significant characteristic of the 24.8-kV system design is a primary selective system for the unit substations [10]–[12]. Figure 4 provides a simplified one-line diagram illustrating this design and shows the line-end and bus-connected VTs of interest. The UPM devices are manually operated, fused, pad-mounted switches. This one line is used for reference in reporting the results of the transient study, ferroresonance analysis, and onsite measurements in this article.



FIGURE 3. A cross section of the line-end VT failure: (a) the VT high-voltage side and (b) the VT windings.

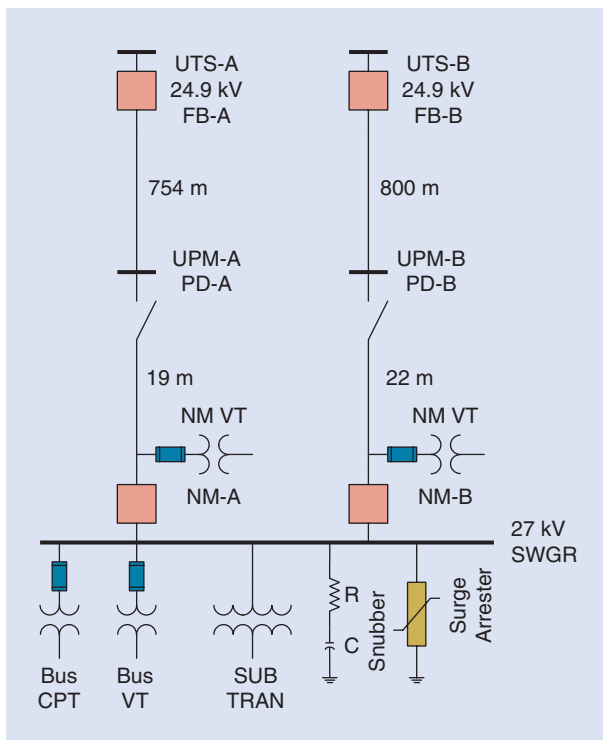


FIGURE 4. A simplified one-line diagram of a typical cell at the data center. R: resistor; C: capacitance; SWGR: switchgear; SUB TRAN: substation transformer; PD: pad-mounted switch.

We conducted a comprehensive investigation of the VT failures by modeling the data center power distribution system, including the switchgear and VTs online and bus-side of the switchgear lineups, and performing a switching transient study to quantify the transient overvoltage produced by the 27-kV breakers at the UTS unit substations.

Using the Alternative Transients Program version of the Electromagnetic Transients Program (EMTP) [13], the medium-voltage distribution system was modeled for switching transient and ferroresonance analysis. Opening of the vacuum circuit breaker (VCB), stray capacitance of the cable, and nonlinear inductance of the VTs being switched (i.e., VT saturation [14], [15]) were represented with sufficient detail.

The study indicated the system was subjected to two different switching phenomena—high-frequency overvoltages and VT ferroresonance. Each issue required its own unique mitigation technique. The high-frequency overvoltages were addressed through implementing a custom resistor–capacitor snubber circuit at each VCB. VT ferroresonance problems are traditionally addressed by the application of a loading resistor across the secondary of the VT to dampen the effects of switching transients. Because the system utilized over 100 VTs, resistor losses over the life of the facility would have been excessive. As an alternative, the problem was addressed through the application of a custom saturable reactor across the secondary of each VT. These solutions are described in more detail in the “Solutions” section.

Baseline testing, without remediation, was performed on 25 February 2014. These results were compared to the snubber/saturable reactor performance testing that was conducted on 3 September 2014 (solution testing). Both tests were conducted by a third party at the facility. The baseline testing was used to characterize the system as it was found and validate the model and resulting transient overvoltages (TOVs) at the line-end and bus VTs, i.e., no additional transient mitigation was installed. The solution testing characterized the system after the installation of custom saturable reactors on the VT secondaries and resulting TOVs at the line-end and bus VTs, i.e., after mitigation was implemented.

Existing System Conditions (Baseline)

A group of sequence operations was performed to cover all operational scenarios of concern. These scenarios were opening and closing the UTS feeder breakers, switching between NM-A and NM-B, and UPM switching activities during various levels of power loading. A set of high-end portable power quality meters were connected to 1,000 : 1 voltage dividers to monitor three medium-voltage points of interest: NM-A line VTs, NM-B line VTs, and the common bus VTs. Another set of identical meters was installed on the secondary side of the NM-A line VTs and the NM-B line VTs. The resultant waveforms were compared for both baseline and solution testing. The waveforms of interest for selected transients are discussed in the following sections.

UTS Breaker Opening During Baseline Testing

During this scenario, a 5-kV square wave at 5–20 Hz was measured during baseline testing. This is very typical of most breaker opening cases, as seen on the bus VT primary shown in Figure 5. Similar results occur when any upstream 27-kV breaker is opened. This is the low-frequency form of ferroresonance associated with VT saturation. The simulation illustrated the worst condition occurred by opening the 27-kV breaker FB-B in switchgear UTS-B with a cable length of 800 m. This case, shown in Figure 6, represents the existing system condition and is the most severe, with the breaker opening time chosen at the phase B maximum voltage. Figures 5 and 6 show a saturation form of ferroresonance, with 5–10-peak kV (kV_{pk}) square waves and an estimated frequency of 17 Hz. The magnitude is well below the normal peak value of 20 kV_{pk} . However, it appears the square wave persists.

Another example of the saturation form of ferroresonance of 5–10 Hz is shown for the UTS breaker FB-A opening during baseline testing, as seen on the bus VT secondary in Figure 7. The simulation illustrates that the worst condition occurs by opening the 27-kV-breaker FB-B in switchgear UTS-B with a cable length of 800 m. This case, shown in Figure 8, represents the existing system condition and shows the VT secondary voltage, the more severe case with the breaker opening time chosen

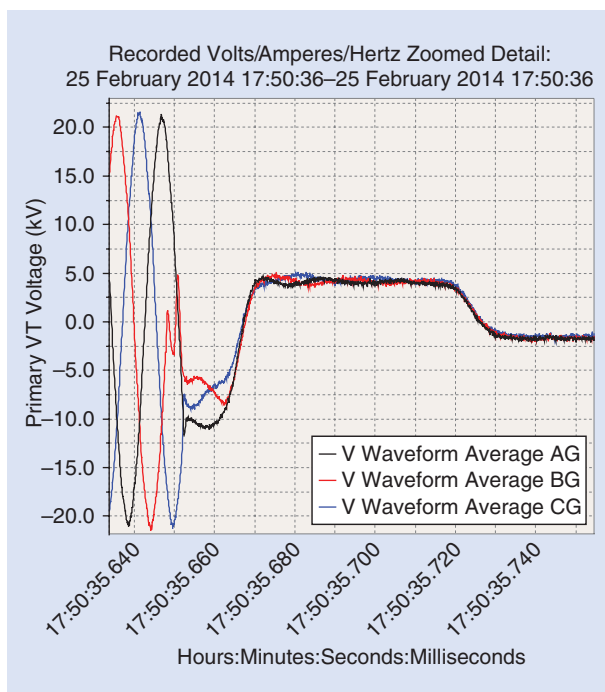


FIGURE 5. The bus VT primary average. AG: phase A to ground; BG: phase B to ground; CG: phase C to ground.

at the phase B maximum voltage. Figures 7 and 8 show a saturation form of ferroresonance, with a 10–30- V_{pk} square wave and an estimated frequency of 5–10 Hz. The magnitude is well below the normal peak value of 100 V_{pk} .

Another example of the saturation form of ferroresonance, during UTS breaker opening, is shown in Figure 9, a saturation 5-kV square wave followed by a sawtooth with six peaks. The figure shows a saturation form of ferroresonance with a 5-k V_{pk} square wave. The sawtooth indicates the line-to-ground voltage coupled through the voltage dividers. The magnitude is well below the normal peak of 20 k V_{pk} .

UPM Switch Closing During Baseline Testing

During the UPM switch closing, a prestrike was captured on the NM-B VT primary transients, as shown in Figure 10. The prestrike shown during breaker closing on all three phases exhibited the highest magnitude, 300 k V_{pk} , at phase C. The prestrike at phase B was a magnitude of 440 k V_{pk} . This is the line-to-ground voltage coupled through the voltage dividers.

During UPM switch closing, a prestrike was captured as seen on the bus VT primary transients (Figure 11). The prestrike occurred during the breaker closing on all three phases; the highest magnitude was 435 k V_{pk} . The prestrike at phase B had a magnitude of 305 k V_{pk} , and the one at phase C had a magnitude of 190 k V_{pk} .

During the UPM switch closing, a prestrike was captured, as seen on the NM-A VT secondary (Figure 12). The prestrike occurred during the switch closing on all

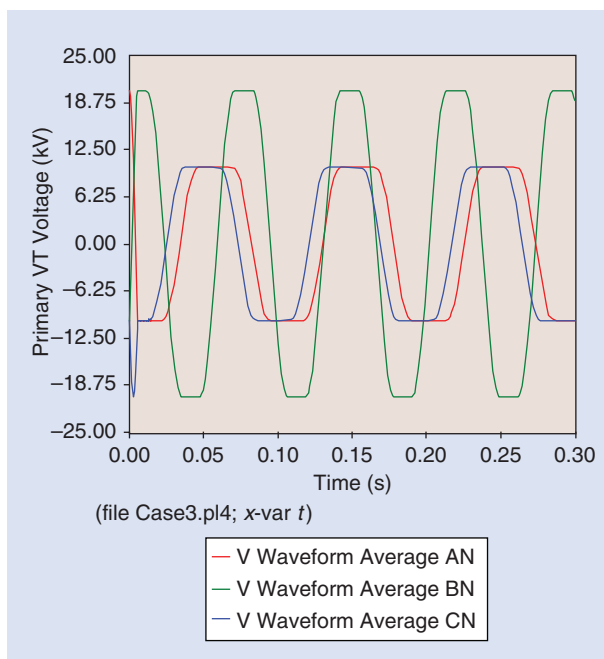


FIGURE 6. The primary line-to-ground voltage after the breaker is opened, illustrating ferroresonance on phase B (from simulation). AN: phase A to neutral; BN: phase B to neutral; CN: phase C to neutral.

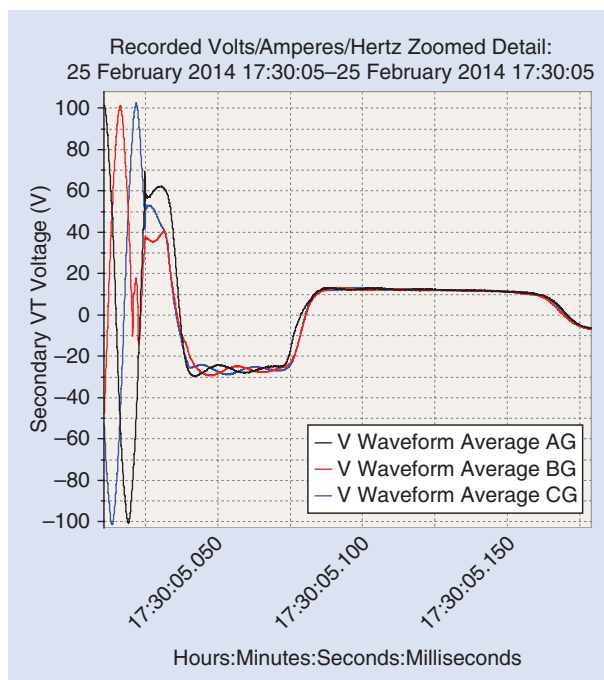


FIGURE 7. The bus VT secondary. AG: phase A to ground; BG: phase B to ground; CG: phase C to ground.

three phases, with the highest magnitude being 500 V_{pk} at phase A. The prestrike at phase C had a magnitude of 135 V_{pk} , and the one at phase B had a magnitude of 260 V_{pk} . This is the line-to-ground voltage capacitively coupled from the primary to the secondary of the VT.

The switch closing case was simulated by closing the UPM switch PD-B upstream of the NM-A VT,

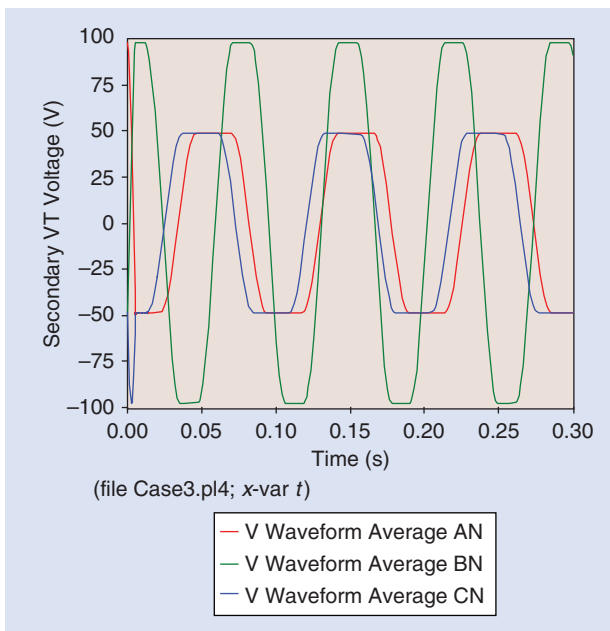


FIGURE 8. The VT secondary voltage after the breaker opens; the ferroresonance is demonstrated from simulation. AN: phase A to neutral; BN: phase B to neutral; CN: phase C to neutral.

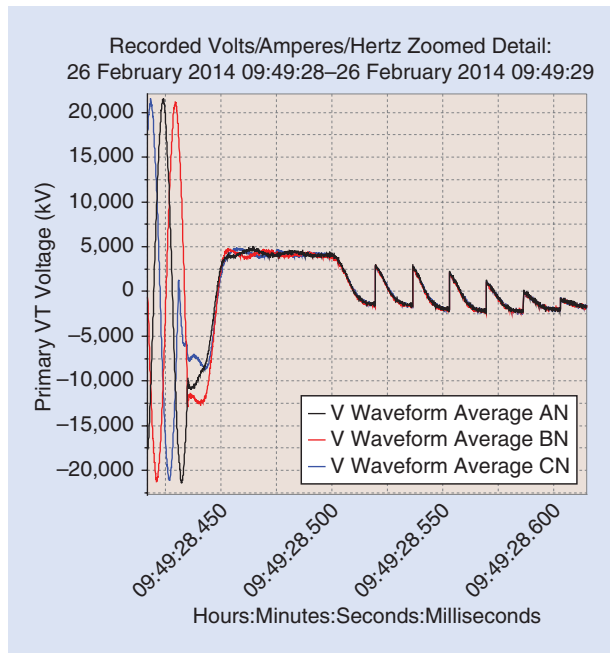


FIGURE 9. The NM-A VT primary, from transients. AN: phase A to neutral; BN: phase B to neutral; CN: phase C to neutral.

with a cable length of 19 m and a pole disagreement of 0.4 ms. Similar to the UPM transient testing, no load was connected at the VT secondary (existing system configuration). Figure 13 shows the line-to-ground TOV is 22.91 kV, with a frequency of 33 kHz. A similar waveform was captured during the energization of a feeder with the NM breaker open. This was typical of all transients observed during the testing, as shown in Figures 14 and 15.

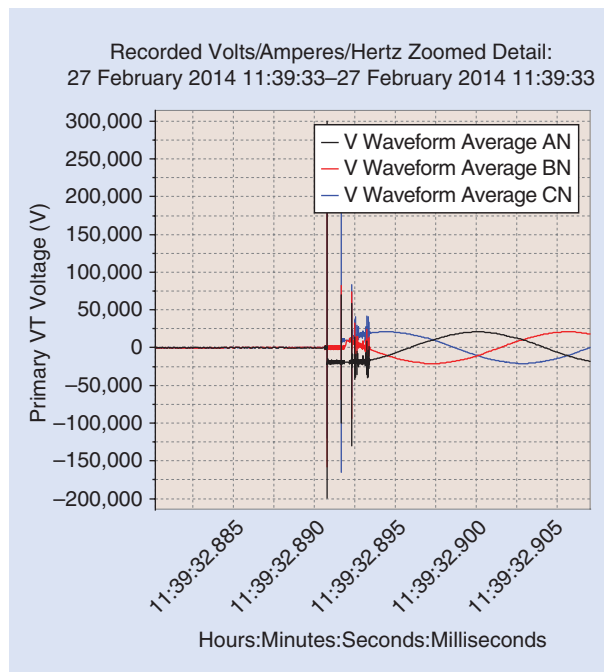


FIGURE 10. The NM-B VT primary, from UPM transients. AN: phase A to neutral; BN: phase B to neutral; CN: phase C to neutral.

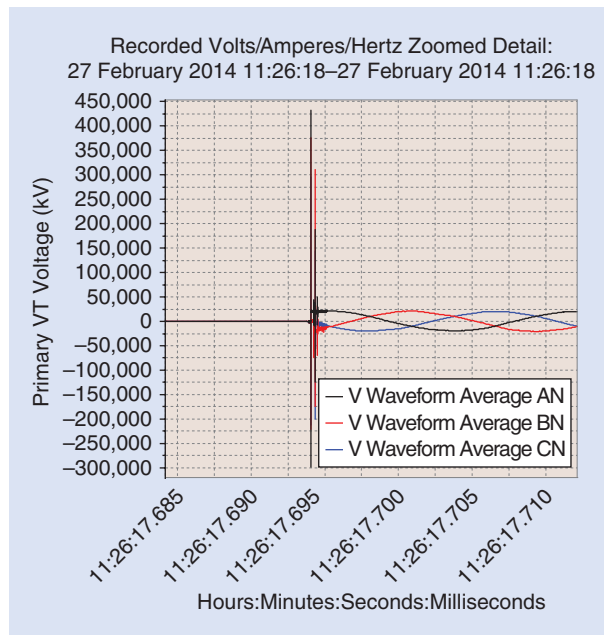


FIGURE 11. The bus VT primary, from baseline testing. AN: phase A to neutral; BN: phase B to neutral; CN: phase C to neutral.

Solutions

The data center’s medium-voltage distribution system was simulated. The following main parameters were modeled for the switching transient and the ferroresonance analysis:

- utility system maximum and minimum fault values
- utility transformers
- cable circuits

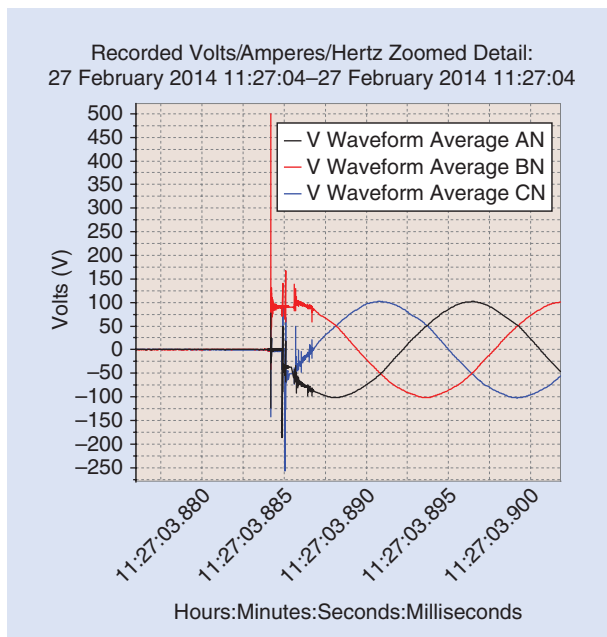


FIGURE 12. The UPM VT secondary, from UPM transients. AN: phase A to neutral; BN: phase B to neutral; CN: phase C to neutral.

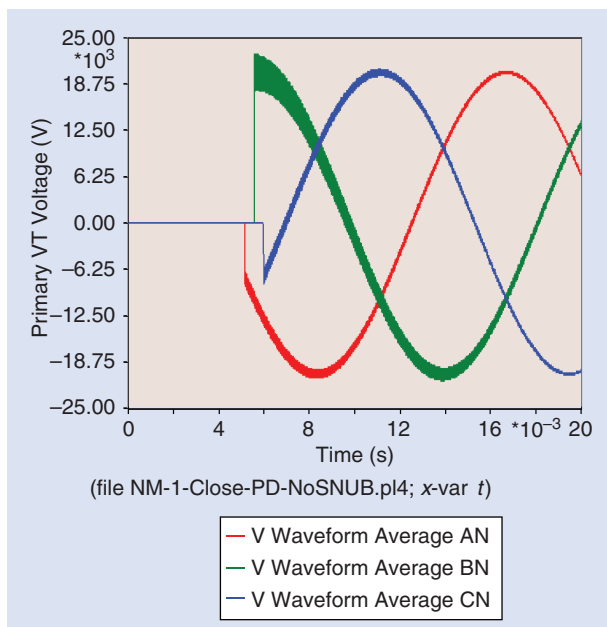


FIGURE 13. The primary line-to-ground voltage after the switch is closed (from simulation). AN: phase A to neutral; BN: phase B to neutral; CN: phase C to neutral.

- equivalent stray capacitance at the switchgear and VTs
- VTs (parameters that include saturation characteristics)
- equivalent stray capacitance across the circuit breaker contacts
- existing surge arrestors
- VCB switching characteristics, including chop current and pole disagreement.

These are common circuit parameters represented in the EMTF model and are usually available from manufacturers, although equivalent stray capacitance

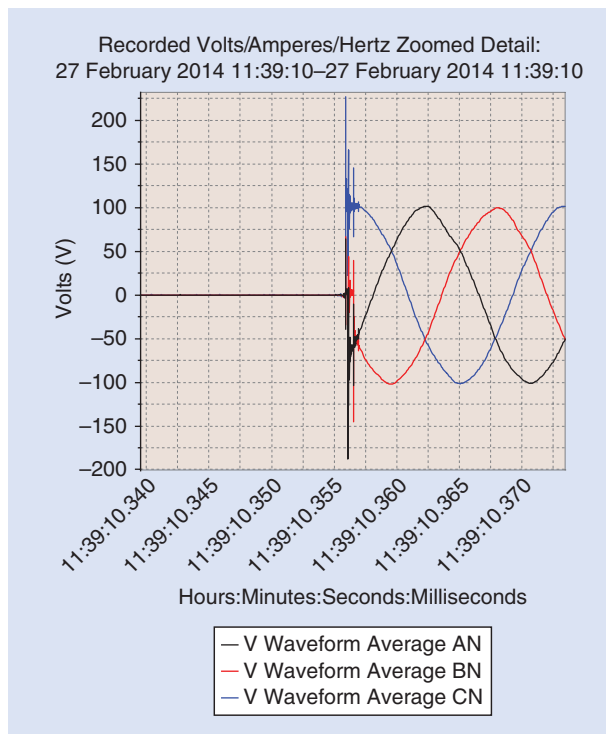


FIGURE 14. The bus VT secondary, from UPM transients. AN: phase A to neutral; BN: phase B to neutral; CN: phase C to neutral.

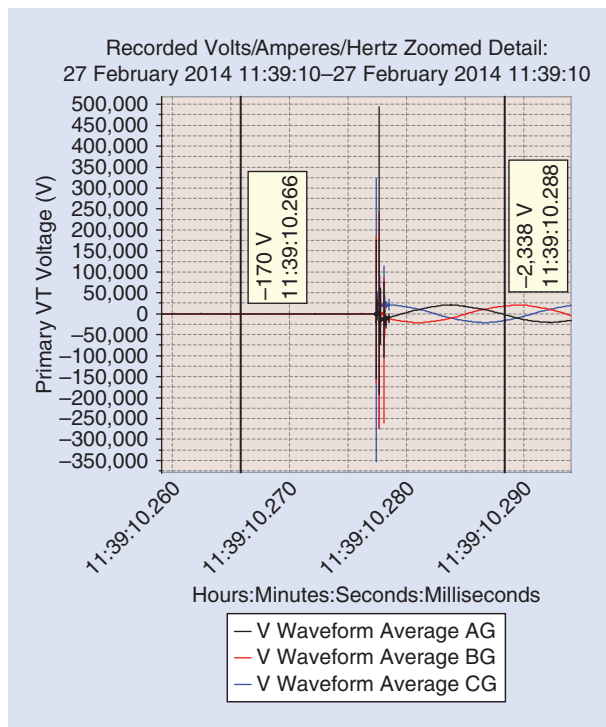


FIGURE 15. A similar scenario to Figure 14, but with a higher voltage transient. AG: phase A to ground; BG: phase B to ground; CG: phase C to ground.

across circuit vacuum breaker contacts is difficult to obtain. When the vacuum interrupter contacts are fully parted inside the vacuum bottle, a capacitance can be measured across the open contacts. Although very small, it will have

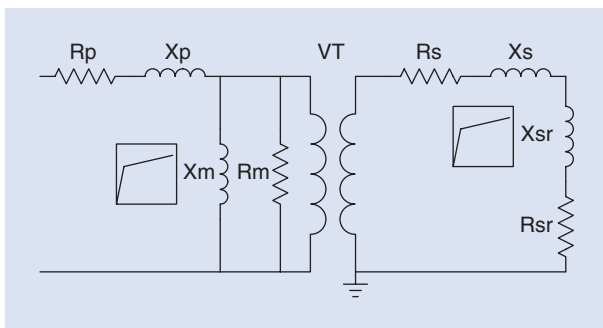


FIGURE 16. The proposed saturable reactor for mitigating VT ferroresonance.

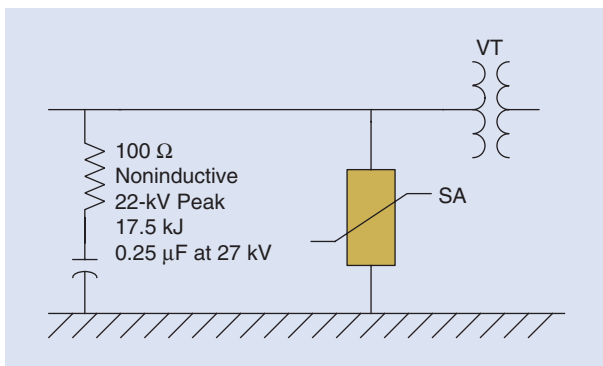


FIGURE 17. The snubber solution for mitigating transient overvoltage at the VT. SA: surge arrester.

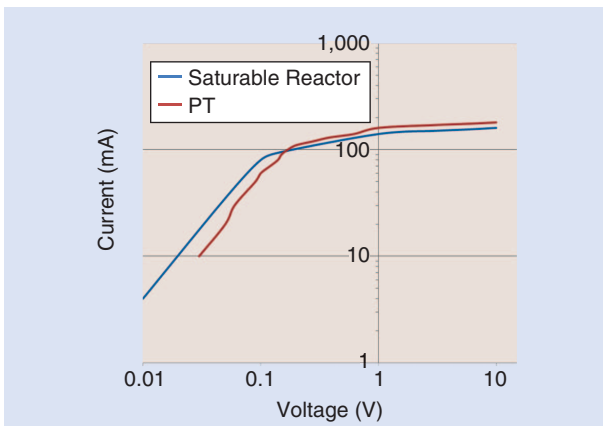


FIGURE 18. A custom saturable reactor designed to mitigate ferroresonance.

an effect on the transient response following the opening of the breaker; this was represented in the simulations.

The simulation results in the “Existing System Conditions (Baseline)” section show that the ferroresonance phenomena occurred for the VTs on the line side of the circuit breakers within the worst ferroresonance locations. A proven solution to ferroresonance is to apply damping resistors to the secondary of the PT. Damping resistors have many advantages, as the resistors are off the shelf, easily available, and provide reasonable damping

times. However, there are disadvantages to the damping resistors: Their burden affects VT accuracy, and they will consume power during the steady state. To counter these disadvantages, switching circuits can be designed to insert the resistor only during ferroresonance. For this data center application, due to the associated power losses and the concern that adding switching circuits may complicate the design, an alternative solution to damping resistors was desired.

A custom-design saturable reactor was proposed and became the subject of this analysis, which forms the basis of this article. This alternative solution requires extensive simulations to custom design the saturation curve for the reactor. It does not affect VT accuracy, has small steady-state losses, and no additional switching circuit is needed, all of which were preferred by the owner of this data center. The simulations show that, with small-reactor resistance, high-speed ferroresonance damping is achieved much faster than the conventional solution of damping resistors.

The proposed and effective solution for mitigating the ferroresonance is a saturable reactor, as shown in Figure 16. After the upstream circuit breaker opens, there will be a dc trapped voltage on the open line. With the VT online side of the downstream breaker, the trapped voltage can be large enough to saturate the VT magnetizing impedance, setting up a resonance condition, which causes the current to oscillate as a square wave. The oscillation can last for an extended period of time, until the eventual failure of the VT. The failure may not necessarily occur based upon just one switching event but can occur over time based upon a number of switching events and where the circuit breaker opens on the voltage waveform [3].

Modeling and site measurements have shown that VCB-induced voltage transients can cause damage to the bus and line VTs because of the short cable lengths. The results of the study indicated that one snubber on the line side of each VT would dramatically reduce the magnitude of the voltage transient as well as its dc offset. The snubber was shown to reduce the frequency of the transient oscillation below the recommended 1,000 Hz. The snubbers were sized per IEEE Standard C57.142-2010 [2], [15]–[17], as shown in Figure 17.

For mitigating the ferroresonance, a custom saturable reactor was created based on the VT saturation curve, as shown in Figure 18. The saturable reactor should be designed to saturate above the VT it is protecting; otherwise it creates a high impedance load on the VT. When the VT sees an overvoltage that goes beyond its thermal rating, which was around 125% of the rated voltage, then the reactor kicks in—but not before. During site testing, the initial reactor design was saturating before the VT. To shift the curve to the right of the VT’s saturation curve, an air gap of about 0.020 cm/in was added. This technique is incorporated in many CTs used

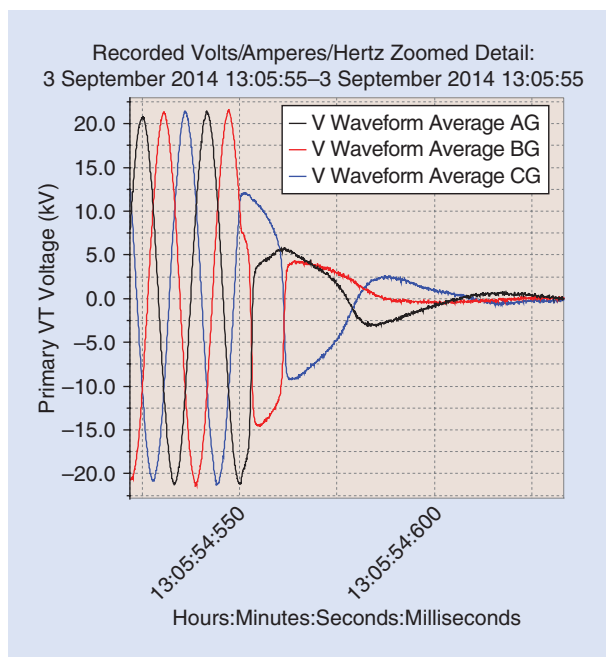


FIGURE 19. The NM-A incoming feeder UTS opening. AG: phase A to ground; BG: phase B to ground; CG: phase C to ground.

for transient performance to reduce remnant (residual magnetism) effects.

The air gap shifted the curve about a decade to the right, which is what was needed from the basic design. It also changed the slope of the linear portion of the curve, which has no bearing on its performance. By adjusting the core size and area as well as the number of turns, no dc component can pass through the VT secondary circuit. The coil resistance was increased by reducing the secondary winding copper area to yield 1Ω . By adding a bifilar winding, an added 5Ω was achieved, but this had zero net effect on flux, inductance, and voltage in the reactor winding. This winding was in series with the main coil to give a net resistance of 6Ω .

Solution Testing

This section shows selected waveforms that prove the effectiveness of the solution. In the “Existing System Conditions (Baseline)” section, tests were performed that show the two problems in the present system configuration. The same testing scenarios will be repeated but after installing/simulating the proposed mitigation; i.e., the VTs are loaded with the saturable reactors and custom snubbers are applied.

UTS Breaker Opening During Solution Testing

As shown in Figure 19, the saturable reactor VT load quickly dampens the ferroresonance to an acceptable level. The simulation results in Figure 20 show similarities to the measured results in Figure 21, and although the simulation case was performed on the most severe case (opening breaker time at the phase B maximum voltage), both cases show damping of

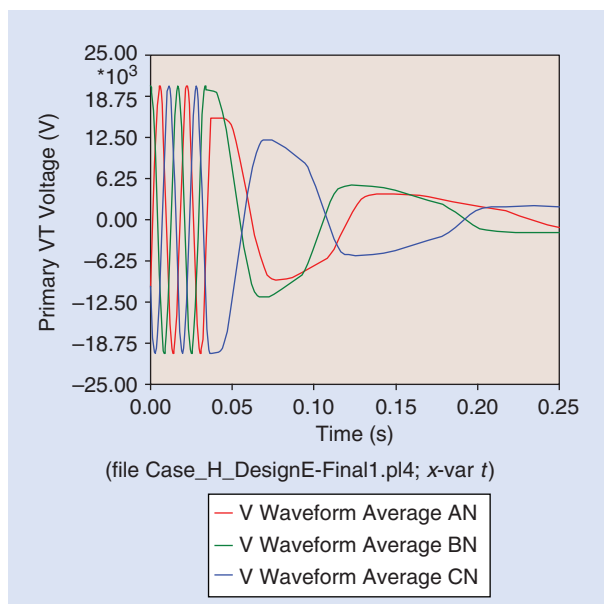


FIGURE 20. The NM-A incoming feeder UTS opening (from simulation). AN: phase A to neutral; BN: phase B to neutral; CN: phase C to neutral.

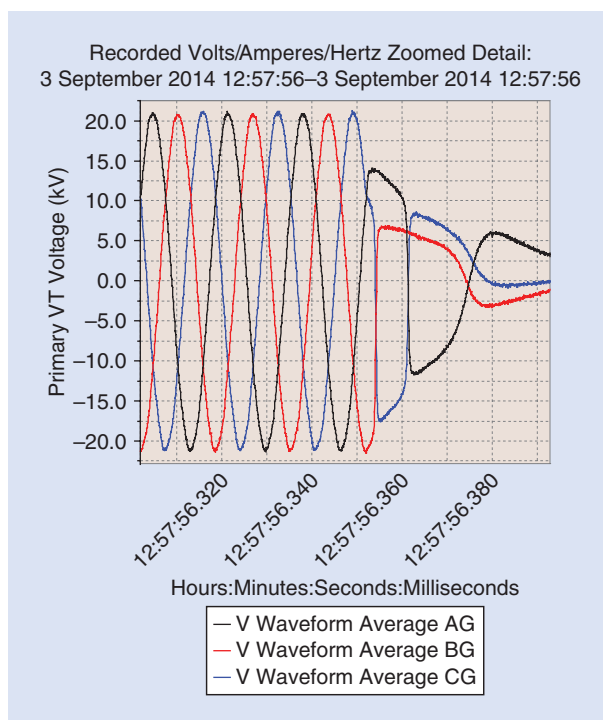


FIGURE 21. The NM-B primary switchgear voltage. AG: phase A to ground; BG: phase B to ground; CG: phase C to ground.

ferroresonance in lower than 250 ms with the saturable reactor installed. This shows the effectiveness of the saturable reactor. Similar waveforms are shown in Figures 21 and 22 for the same switching event of opening the upstream UTS breaker. As shown in Figures 20–22, the damping time is lower than 100 ms, and the voltage magnitude is in the normal peak value of 20 kV.

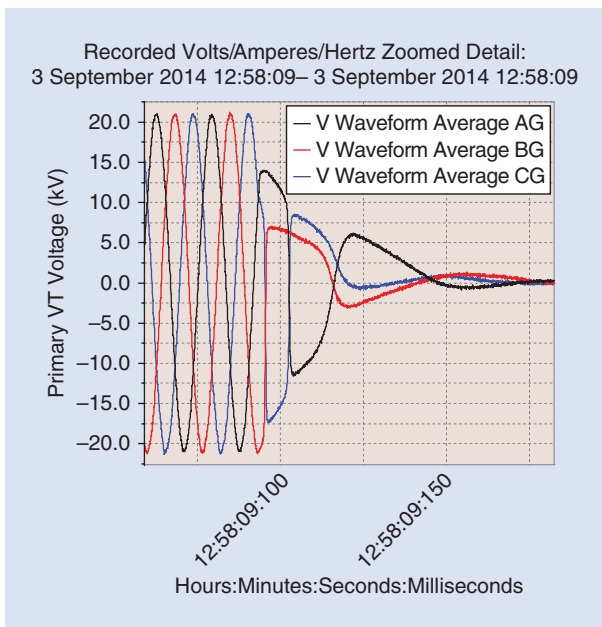


FIGURE 22. The bus primary voltage after UTS opening. AG: phase A to ground; BG: phase B to ground; CG: phase C to ground.

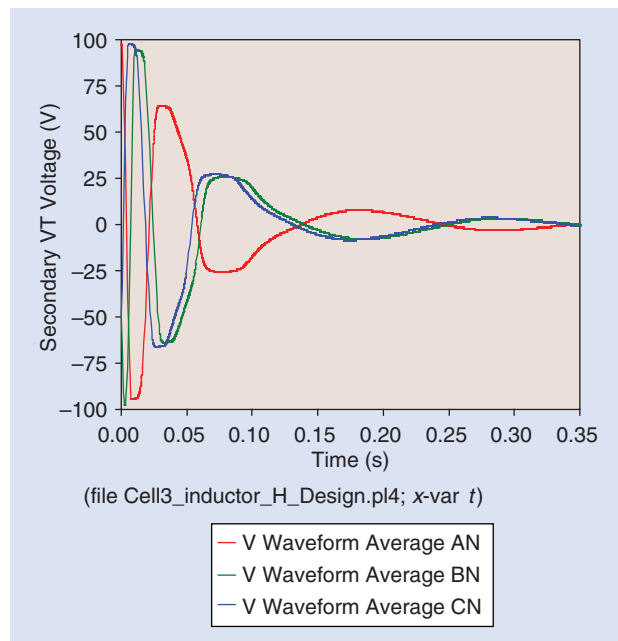


FIGURE 24. The NM-A secondary voltage after UTS opening (from simulation). AN: phase A to neutral; BN: phase B to neutral; CN: phase C to neutral.

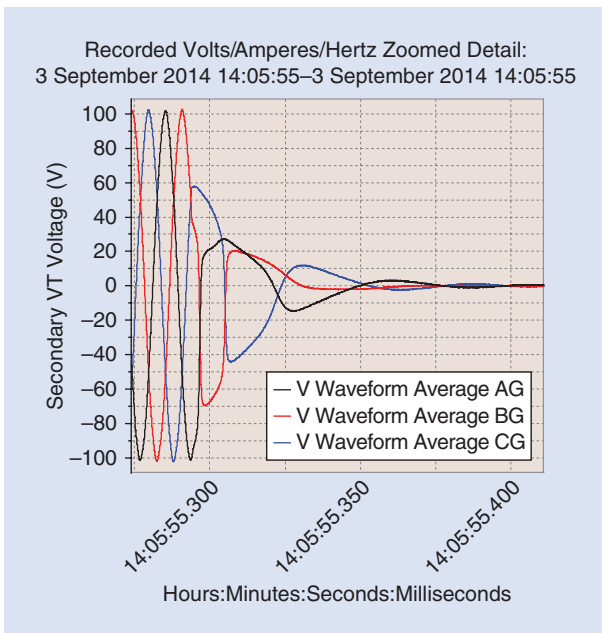


FIGURE 23. The NM-A secondary voltage after UTS opening. AG: phase A to ground; BG: phase B to ground; CG: phase C to ground.

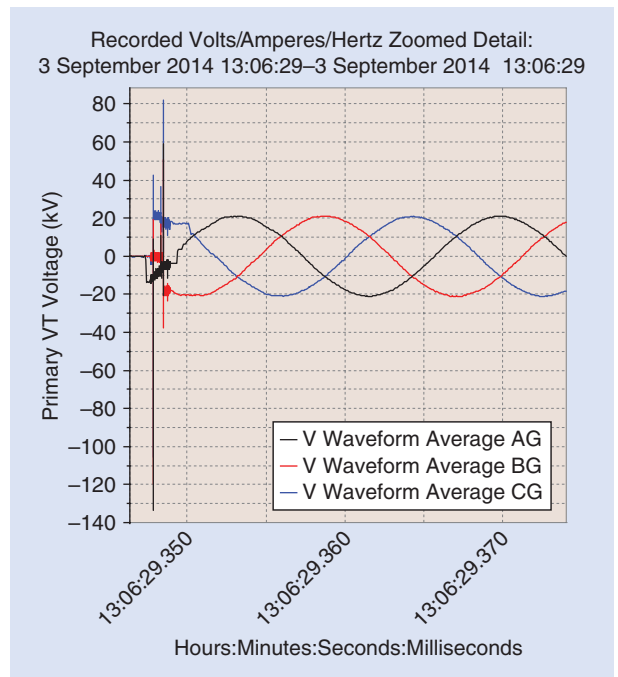


FIGURE 25. The NM-A primary VT voltage. AG: phase A to ground; BG: phase B to ground; CG: phase C to ground.

In Figures 23 and 24, after opening breaker FB-A, secondary VT waveforms are shown. Figure 23 shows the NM-A secondary voltage, and Figure 24 shows the simulated VT secondary voltage. The simulated case shows the worst case, but both show damping in fewer than 250 ms.

UPM Switch Closing During Solution Testing

This section discusses similar testing conditions as in the previous section, except custom snubbers were installed

at the primary of the VTs. During closing, as performed in the “Existing System Conditions (Baseline)” section (closing the UPM switch PD-A upstream), prestrike was captured as seen on NM-A and NM-B VT primaries and in Figures 25 and 26; these figures also show that the TOV was damped quickly after closing the upstream switch and that the voltage magnitude is in the normal peak value of 140 kV.

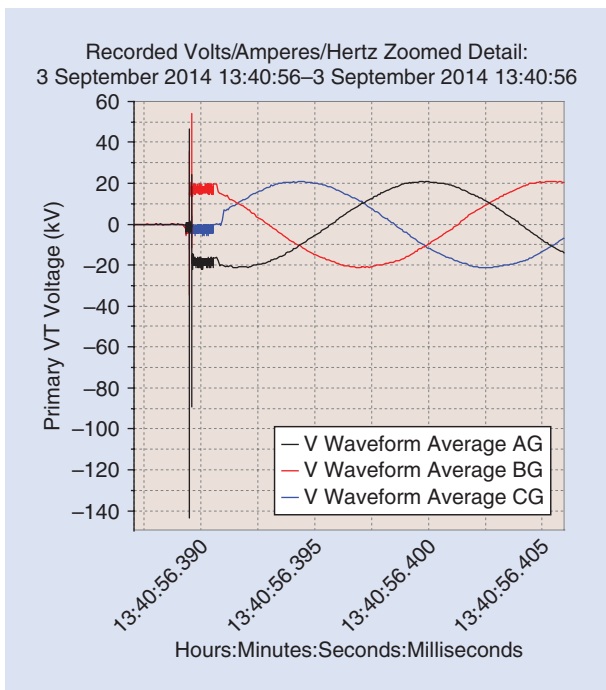


FIGURE 26. The NM-B primary voltage. AG: phase A to ground; BG: phase B to ground; CG: phase C to ground.

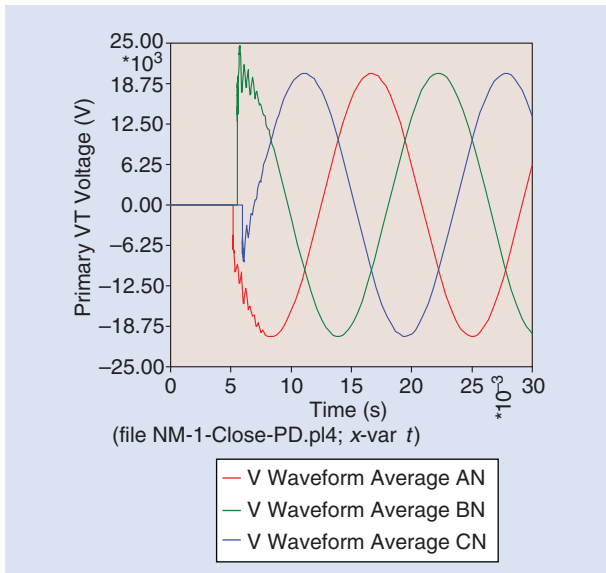


FIGURE 27. The NM-A primary VT voltage after closing the UPM switch using a snubber (from simulation). AN: phase A to neutral; BN: phase B to neutral; CN: phase C to neutral.

This case was again simulated by closing the upstream UPM switch PD-A. The TOV magnitude was 24.67 kV, with a frequency of 3,300 Hz, as shown in Figure 27. Note that the case was initially simulated in EMTF with a 30-Ω resistor and 0.125 μF capacitor. The case was repeated using a fine-tuned snubber (100 Ω and 0.25 μF). This showed a reduced TOV of 26.14 kV, with a frequency of 2,500 Hz, as shown in Figure 28.

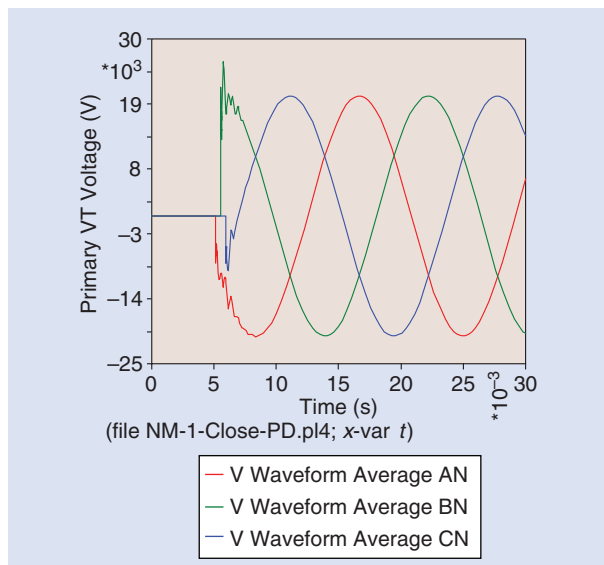


FIGURE 28. The NM-A primary VT voltage after closing the UPM switch (from simulation). AN: phase A to neutral; BN: phase B to neutral; CN: phase C to neutral.

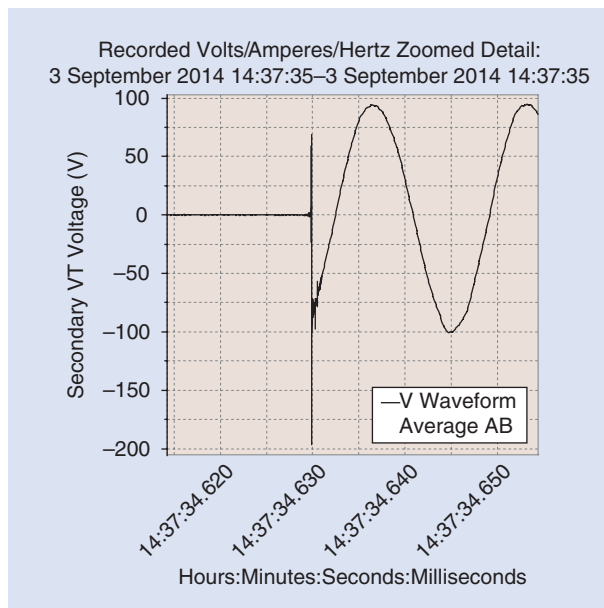


FIGURE 29. The bus VT secondary voltage after UPM switching.

Figures 29 and 30 show the VT secondary voltage when closing the UPM PD-B switch. In Figure 30, notice that phase A closes first, followed by a very small delay when phase B closes, and then a much longer delay until phase C closes. This pole separation or pole disagreement can initiate transients in the other phases for which the pole has not yet opened. In both phases A and B, there is a significant TOV followed by a damped oscillation. The peak as well as the rate of change of voltage can damage the VT primary winding insulation.

This case was simulated by closing the UPM switch PD-B upstream. The TOV magnitude is 120.01 V with a

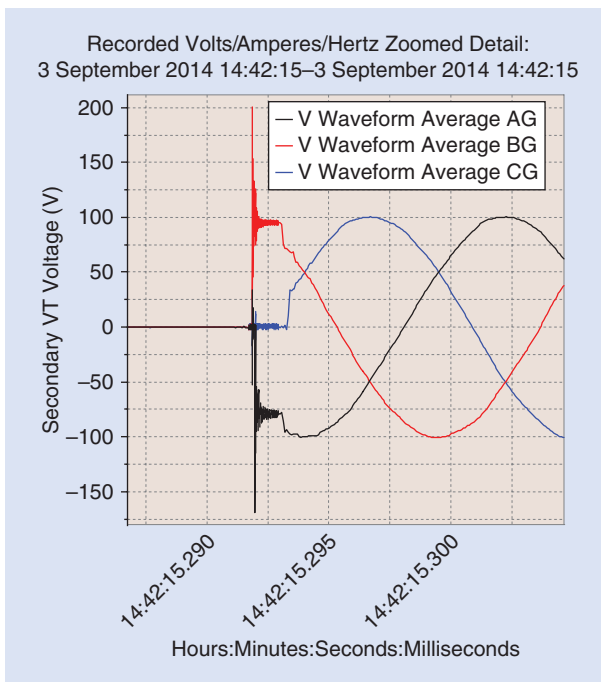


FIGURE 30. The secondary bus voltage after closing the NM-B. AG: phase A to ground; BG: phase B to ground; CG: phase C to ground.

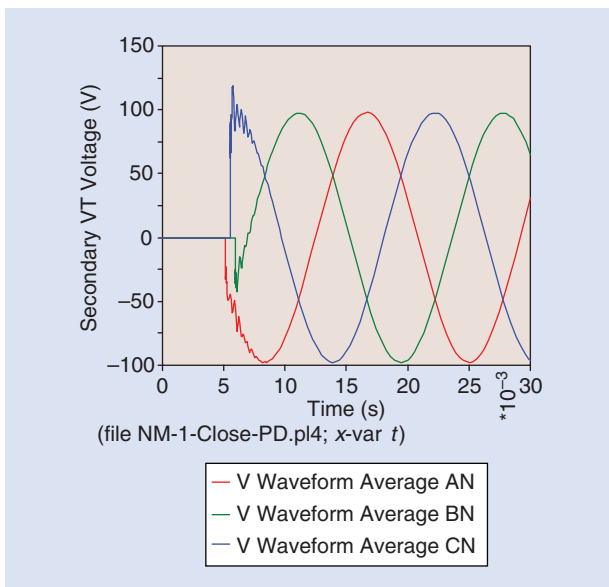


FIGURE 31. The NM-A secondary VT voltage after closing the UPM switch using an off-shelf snubber (from simulation). AN: phase A to neutral; BN: phase B to neutral; CN: phase C to neutral.

frequency of 3,300 Hz, as shown in Figure 31. Note that the case was initially simulated with a 30-Ω resistor and a 0.125 μF capacitor, but repeated using a fine-tuned snubber (100 Ω and 0.25 μF). This analysis shows a reduced TOV of 125.52 V, with a frequency of 2,500 Hz, as shown in Figure 32. There is a reduction in the TOV by using the fine-tuned snubber, but it still damped to an acceptable level.

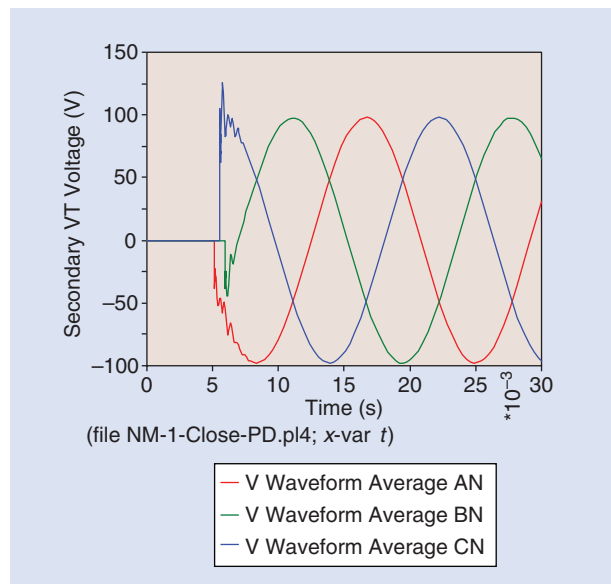


FIGURE 32. The NM-A secondary VT voltage after closing the UPM switch. AN: phase A to neutral; BN: phase B to neutral; CN: phase C to neutral.

Conclusions and Observations

The “Existing System Conditions (Baseline)” and “Solution Testing” sections have shown the resultant waveforms during the UTS breaker opening and closing with and without the saturable reactor as a solution to the ferroresonance problem and with and without custom snubbers as a solution to the switching transient problem. The effectiveness of the implemented solution has been verified through field testing and simulation. During baseline testing, the measured waves showed significant 5–20-Hz ferroresonance at the VT on opening and even worse pre-strike/reignition transients on closing. After the installation of saturable reactors, the system settles quickly for the same tests, i.e., in fewer than 100 ms. It has been clearly shown that the saturable reactors provide the necessary damping to mitigate the ferroresonance problem at this data center.

On breaker closing during both baseline and solution testing, the transients on the primary of the VTs showed significant magnitude, on the order of 500 kV, with pole disagreement of about 1 ms. The corresponding transient on the VT secondary was on the order of 500 V. The transients are capacitively coupled from the primary to secondary of the VT, not through the turns ratio, so the voltage divider scaling/calibration is not a concern.

For the breaker closing during both baseline and solution testing, there were many prestrike events. Similar prestrike events have been observed for a VCB closing into an arc furnace transformer. In that case, the prestrike was aggravated when the operators opened and closed the VCB about five times within as many minutes. For the testing at this data center, the iterations of breaker close/open of up to six times may not have allowed the vacuum

interrupter to fully recover, resulting in prestrike on the next close operation.

On breaker opening during baseline testing, there is evidence of a saturation form of ferroresonance. After the breaker opens, there is a pronounced square wave of 5 kV, with a frequency of 5–20 Hz as seen at the VT primary. This response is very typical of the breaker opening cases. The square wave persists for a few cycles at 5–10 Hz before damping out. During solution testing, the system shows a fast damping of oscillations within 100 ms. However, in at least one case during baseline testing, the saturation form of ferroresonance square wave had a much higher magnitude of 75 V at 4 Hz, as seen at the VT secondary. This higher magnitude was preceded by reignition during breaker opening on all three phases. The reignition may have trapped an additional charge, increasing the voltage on the secondary of the VT.

During the opening of the NM-B breaker (baseline testing), transients were noted at the NM-A VT on the order of 475 kV_{pk}. This is significant because the NM-A breaker was already open by this point. The transient was coupled from NM-B up through the 24.5-kV UTS feeder and back down through the adjacent UTS feeder to NM-A.

The magnitude of the TOVs during baseline and solution testing on the order of 500 kV_{pk} and rate of rise reported on the primary of the VTs would be expected to cause the surge arrester to operate, but it did not. It is possible that there was a scaling/calibration issue between the voltage dividers and the power quality meter. The voltage dividers have a ratio of 1,000 : 1, which gives 20-Vrms line-to-ground input to the power quality meter. The power quality meter has a minimum input voltage of 60 V. The transient response of the power quality meter in the 20-V range is not known. Normally the power quality meter is applied at 120/208 V or 277/480 V, which results in input voltages well above the minimum of 60 V.

Author Information

Tamer Abdelazim Mellik (abdelazim@ieee.org) is with the Eaton Corporation Power Systems Engineering, Calgary, Canada. **Thomas J. Dionise** is with Eaton Corporation Power Systems Engineering, Warrendale, Pennsylvania. **Robert Yanniello** is with Eaton Corporation, Arden, North Carolina. Mellik is a Senior Member of the IEEE.

This article first appeared as “A Case Study of Voltage Transformer Failures in a Modern Data Center: Analysis, Mitigation, and Solution Implementation” at the 2016 IEEE IAS 52nd Industrial and Commercial Power Systems Technical Conference. This article was reviewed by the IAS Power Systems Protection Committee.

References

- [1] *A Guide to Describe the Occurrence and Mitigation of Switching Transients Induced By Transformer And Switching Device Interaction*, ANSI/IEEE Standard C57.142-2010, Apr. 2011.
- [2] D. Shipp, T. Dionise, V. Lorch, and B. MacFarlane, “Transformer failure due to circuit breaker induced switching transients,” *IEEE Trans. Ind. Appl.*, vol. 47, no. 2, pp. 707–718, Apr./May 2011.
- [3] D. Shipp, T. Dionise, V. Lorch and D. McDermit, “Medium voltage switching transient induced potential transformer failures; prediction, measurement and practical solutions,” *IEEE Trans. Ind. Appl.*, pp. 1726–1737, July/Aug. 2013.
- [4] D. Shipp and R. Hoerauf, “Characteristics and applications of various arc interrupting methods,” *IEEE Trans. Ind. Appl.*, vol. 27, pp. 849–861, Sept./Oct 1991.
- [5] *IEEE Standard for AC High-Voltage Generator Circuit Breakers on a Symmetrical Current Basis*, ANSI/IEEE Standard C37.013-1997, Dec. 1997.
- [6] *IEEE Guide for the Application of Transient Recovery Voltage for AC High-Voltage Circuit Breakers*, ANSI/IEEE Standard C37.011-2011, Nov. 2011.
- [7] D. Durocher, “Considerations in unit substation design to optimize reliability and electrical workplace safety,” in *Proc. Industrial and Commercial Power Systems Technical Conference (I&CPS)*, Tallahassee, FL, May 2010, pp. 1–11.
- [8] *IEEE Standard Dictionary of Electrical and Electronics Terms*, ANSI/IEEE Standard 100-1972.
- [9] R. H. Hopkinson, “Ferroresonant overvoltages due to open conductors,” *General Electric Publication*, 1967, pp. 3–6.
- [10] Westinghouse Electric Corp., Distribution Transformer Division, “Ferroresonance,” in *Westinghouse Distribution Transformer Guide*. Athens, GA: Westinghouse Electric Corporation, Apr. 1986, pp. 36–40.
- [11] *IEEE Guide for Application of Transformers*, ANSI/IEEE Standard C57.105-1978, 2008.
- [12] Ontario Hydro, *Distribution Technical Guide*. Ontario, Canada: Ontario Hydro, May 1999, pp. 72.1-1–72.1-10.
- [13] Alternative Transients Program. (2015). Welcome to EEUG, users group of ATP-EMTP. *EEUG*. [Online]. Available: <http://eeug-test.hostingkunde.de/>
- [14] A. Greenwood, *Electrical Transients in Power Systems*. New York: Wiley, 1971, pp. 91–93.
- [15] L. Kojovic and A. Bonner, “Ferroresonance—Culprit and scapegoat,” *Cooper Power Systems, The Line*, Dec. 1998.
- [16] *IEEE Guide to Describe the Occurrence and Mitigation of Switching Transients Induced by Transformers, Switching Device, and System Interaction*, ANSI/IEEE Standard C57.142-2010, Apr. 2011.
- [17] C. S. Mardegan, D. D. Shipp, L. A. R. Melo, M. R. Santana, “The experience acquired sizing snubbers to mitigate switching transients in industrial power systems,” in *Proc. IEEE IAS I&CPS Conference*, May 2015, pp. 1–10.

